2003

Phase Transformation Driven by Valence Electron Concentration: Tuning Interslab Bond Distances in Gd5GaxGe4-x

Yurij Mozharivskyj
Iowa State University

Wonyoung Choe
Lawrence Livermore National Laboratory

Alexandra O. Pecharsky
Iowa State University

Gordon J. Miller
Iowa State University, gmiller@iastate.edu

Phase Transformation Driven by Valence Electron Concentration: Tuning Interslab Bond Distances in Gd5GaxGe4-x

Abstract

X-ray single crystal and powder diffraction studies on the $Gd_5Ga_xGe_{4-x}$ system with $0 \le x \le 2.2$ reveal dependence of interslab T−T dimer distances and crystal structures themselves on valence electron concentration (T is a mixture of Ga and Ge atoms). While the $Gd_5Ga_xGe_{4-x}$ phases with $0 \le x \le 0.6$ and valence electron concentration of 30.4−31 e^-/formula crystallize with the Sm_5Ge_4-type structure, in which all interslab T−T dimers are broken (distances exceeding 3.4 Å), the phases with $1 \le x \le 2.2$ and valence electron concentration of 28.8−30 e-/formula adopt the Pu_5Rh_4- or Gd_5Si_4-type structures with T−T dimers between the slabs. An orthorhombic Pu_5Rh_4-type structure, which is intermediate between the Gd_5Si_4- and Sm_5Ge_4-type structures, has been identified for the Gd_5GaGe_3 composition. Tight-binding linear-muffin-tin-orbital calculations show that substitution of three-valent Ga by four-valent Ge leads to larger population of the antibonding states within the dimers and, thus, to dimer stretching and eventually to dimer cleavage.

Disciplines

Materials Chemistry | Other Chemistry | Physical Chemistry

Comments

Reprinted (adapted) with permission from J. Am. Chem. Soc., 2003, 125 (49), pp 15183–15190.

J|A|C|S
ARTICLES
Published on Web 11/12/2003

Phase Transformation Driven by Valence Electron Concentration: Tuning Interslab Bond Distances in $Gd_5Ga_xGe_{4-x}$

Yurij Mozharivskyj,[†] Wonyoung Choe,[‡] Alexandra O. Pecharsky,[†] and Gordon J. Miller*[,§]

Contribution from the Ames Laboratory, Iowa State University, Ames, Iowa 500110, Lawrence Livermore National Laboratory, L-418, Livermore, California 94550, and the Department of Chemistry, Iowa State University, Ames, Iowa 50011

Received July 30, 2003; E-mail: gmiller@iastate.edu

Abstract: X-ray single crystal and powder diffraction studies on the $Gd_5Ga_xGe_{4-x}$ system with $0 \le x \le 2.2$ reveal dependence of interslab T−T dimer distances and crystal structures themselves on valence electron concentration (T is a mixture of Ga and Ge atoms). While the $Gd_5Ga_xGe_{4-x}$ phases with $0 \le x \le 0.6$ and valence electron concentration of 30.4−31 e^-/formula crystallize with the Sm_5Ge_4-type structure, in which all interslab T−T dimers are broken (distances exceeding 3.4 Å), the phases with $1 \le x \le 2.2$ and valence electron concentration of 28.8−30 e-/formula adopt the Pu_5Rh_4- or Gd_5Si_4-type structures with T−T dimers between the slabs. An orthorhombic Pu_5Rh_4-type structure, which is intermediate between the Gd_5Si_4- and Sm_5Ge_4-type structures, has been identified for the Gd_5GaGe_3 composition. Tight-binding linear-muffin-tin-orbital calculations show that substitution of three-valent Ga by four-valent Ge leads to larger population of the antibonding states within the dimers and, thus, to dimer stretching and eventually to dimer cleavage.

Introduction

Recent discovery of the giant magnetocaloric effect in $Gd_5Si_2Ge_2$[1−3] triggered extensive research in the R_5X_4 systems (R is a rare-earth element and X is a main group element).[4−16] Interest in these materials is fueled by economic benefits, i.e., potential application of $Gd_5Si_2Ge_2$[17−20] for room-temperature magnetic refrigeration with larger efficiency than current vapor-cycle units, as well as by scientific curiosity, directed toward understanding this unusual phenomenon.[21−24] The magnetic ordering in $Gd_5Si_2Ge_2$ is coupled with a reversible, first-order structural transformation: the low-temperature ferromagnetic form adopts an orthorhombic Gd_5Si_4-type structure with T−T dimers between $_\infty^2[Gd_5T_4]$ slabs (T is a statistical mixture of Ge and Si atoms on the corresponding sites), and the room-temperature paramagnetic form has a monoclinic $Gd_5Si_2Ge_2$-type structure, in which half of the T−T interslab dimers are broken.[21] This magnetic/martensitic transition can be controlled by changing composition, temperature, pressure, and magnetic field.[21,23,25]

One of the interesting features of the transformation is that the low-temperature phase has a higher symmetry (*Pnma* space group) than the room-temperature phase ($P11_2/a$ space group). Calculations by Choe et al.[21] and later by Pecharsky et al.[26]

[†] Ames Laboratory, Iowa State University.
[‡] Lawrence Livermore National Laboratory.
[§] Department of Chemistry, Iowa State University.

(1) Pecharsky, V. K.; Gschneidner, K. A., Jr. *J. Alloys Compd.* **1997**, *260*, 98.
(2) Pecharsky, V. K.; Gschneidner, K. A., Jr. *Phys. Rev. Lett.* **1997**, *78*, 4494.
(3) Pecharsky, V. K.; Gschneidner, K. A., Jr. *J. Magn. Magn. Mater.* **1997**, *167*, L179.
(4) Pecharsky, V. K.; Gschneidner, K. A., Jr. *J. Appl. Phys.* **1999**, *86*, 6315.
(5) Ivtchenko, V. V.; Pecharsky, V. K.; Gschneidner, K. A., Jr. *Adv. Cryog. Eng.* **2000**, *46*, 405.
(6) Gschneidner, K. A., Jr.; Pecharsky, V. K.; Pecharsky, A. O.; Ivtchenko, V. V.; Levin, E. M. *J. Alloys Compd.* **2000**, *303*−*304*, 214.
(7) Levin, E. M.; Gschneidner, K. A., Jr.; Pecharsky, V. K. *J. Magn. Magn. Mater.* **2001**, *231*, 135.
(8) Levin, E. M.; Gschneidner, K. A., Jr.; Pecharsky, V. K. *Phys. Rev. B* **2002**, *65*, 214 427.
(9) Huang, H.; Pecharsky, A. O.; Pecharsky, V. K.; Gschneidner, K. A., Jr. *Adv. Cryog. Eng.* **2002**, *48*, 11.
(10) Pecharsky, V. K.; Pecharsky, A. O.; Mozharivskyj, Y.; Gschneidner, K. A.; Miller, G. J. *Physical Review Lett.*, submitted.
(11) Wang, H. B.; Altounian, Z.; Ryan, D. H. *Phys. Rev. B* **2002**, *66*, 214 413.
(12) Cadogan, J. M.; Ryan, D. H.; Altounian, Z.; Wang, H. B.; Swainson, I. P. *J. Phys.: Condens. Matter* **2002**, *14*, 7191.
(13) Yang, H. F.; Rao, G. H.; Liu, G. Y.; Ouyang, Z. W.; Feng, X. M.; Liu, W. F.; Chu, W. G.; Liang, J. K. *J. Phys.: Condens. Matter* **2002**, *14*, 9705.
(14) Yang, H. F.; Rao, G. H.; Liu, G. Y.; Ouyang, Z. W.; Liu, W. F.; Feng, X. M.; Chu, W. G.; Liang, J. K. *J. Alloys Compd.* **2002**, *346*, 190.
(15) Yang, H. F.; Rao, G. H.; Liu, G. Y.; Ouyang, Z. W.; Liu, W. F.; Feng, X. M.; Chu, W. G.; Liang, J. K. *Physica B (Amsterdam)* **2003**, *325*, 293.
(16) Yang, H. F.; Rao, G. H.; Liu, G. Y.; Ouyang, Z. W.; Liu, W. F.; Feng, X. M.; Chu, W. G.; Liang, J. K. *J. Alloys Compd.* **2003**, *348*, 150.
(17) Gschneidner, K. A., Jr.; Pecharsky, V. K. *Annu. Rev. Mater. Sci.* **2000**, *30*, 387.
(18) Pecharsky, V. K.; Gschneidner, K. A., Jr. *Adv. Mater.* **2001**, *13*, 683.
(19) Gschneider, K. A., Jr.; Pecharsky, V. K. *Intermet. Compd.* **2002**, *3*, 519.
(20) Gschneidner, K. A., Jr.; Pecharsky, A. O.; Pecharsky, V. K.; Lograsso, T. A.; Schlagel, D. L. In *Rare Earths and Actinides: Science, Technology and Applications IV.*, Proceedings of Symposium held during the TMS Annual Meeting: Nashville, TN, United States, Mar. 12−16, 2000, pp 63−72.
(21) Choe, W.; Pecharsky, V. K.; Pecharsky, A. O.; Gschneidner, K. A., Jr.; Young, V. G., Jr.; Miller, G. J. *Phys. Rev. Lett.* **2000**, *84*, 4617.
(22) Levin, E. M.; Pecharsky, A. O.; Pecharsky, V. K.; Gschneidner, K. A., Jr. *Phys. Rev. B* **2001**, *63*, 064 426.
(23) Pecharsky, A. O.; Gschneidner, K. A., Jr.; Pecharsky, V. K.; Schindler, C. E. *J. Alloys Compd.* **2002**, *338*, 126.
(24) Meyers, J.; Chumbley, S.; Choe, W.; Miller, G. J. *Phys. Rev. B* **2002**, *66*, 012 106.
(25) Morellon, L.; Algarabel, P. A.; Ibarra, M. R.; Blasco, J.; Garcia-Landa, B.; Arnold, Z.; Albertini, F. *Phys. Rev. B* **1998**, *58*, R14 721.
(26) Pecharsky, V. K.; Samolyuk, G. D.; Antropov, V. P.; Pecharsky, A. O.; Gschneidner, K. A., Jr. *J. Solid State Chem.* **2003**, *171*, 57.

Table 1. Crystallographic Data for $Gd_5Ga_xGe_{4-x}$ Powders and Single Crystals

x	sample	str. type of phases	*a*, Å	*b*, Å	*c*, Å	c/a	*V*, Å^3
0	powder	Sm_5Ge_4	7.6939(3)	14.8232(6)	7.7825(3)	1.01152(5)	887.6(1)
	crystal	Sm_5Ge_4	7.683(2)	14.811(4)	7.774(2)	1.0118(3)	884.6(4)
0.5	powder	Sm_5Ge_4	7.679(6)	14.87(1)	7.808(4)	1.0168(9)	892(1)
	crystal	Sm_5Ge_4	7.660(1)	14.860(3)	7.811(2)	1.0197(3)	889.2(3)
0.6	powder	Sm_5Ge_4	7.6598(6)	14.879(1)	7.8141(5)	1.0201(1)	890.6(1)
0.7	powder[a]	$Sm_5Ge_4 + Pu_5Rh_4$	7.563(7)	14.88(1)	7.88(1)	1.042(2)	887(1)
	crystal	Sm_5Ge_4[b] $+ Pu_5Rh_4$	7.6195(8)	14.838(2)	7.8162(8)	1.0258(3)	883.7(2)
0.8	powder[a]	$Sm_5Ge_4 + Pu_5Rh_4$	7.5518(5)	14.896(4)	7.8894(6)	1.0447(1)	887.5(3)
	crystal	Sm_5Ge_4[b] $+ Pu_5Rh_4$	7.613(1)	14.880(3)	7.846(2)	1.0306(3)	888.7(3)
0.9	powder[a]	$Sm_5Ge_4 + Pu_5Rh_4$	7.5438(3)	14.892(8)	7.8827(4)	1.04492(7)	885.6(5)
1	powder	Pu_5Rh_4	7.5473(2)	14.9217(9)	7.8951(5)	1.04608(9)	889.1(1)
	crystal	Pu_5Rh_4	7.572(2)	14.933(3)	7.884(2)	1.0412(3)	891.5(3)
1.2	powder	Gd_5Si_4	7.5348(3)	14.9485(4)	7.9046(4)	1.04908(7)	890.3(1)
1.5	powder	Gd_5Si_4	7.5234(3)	14.9892(6)	7.9183(3)	1.05249(6)	892.9(1)
2	powder	Gd_5Si_4	7.5226(4)	15.0068(8)	7.9275(4)	1.05382(8)	894.9(1)
	crystal	Gd_5Si_4	7.5162(7)	14.971(1)	7.9149(7)	1.0531(1)	890.6(1)
2.2	powder	Gd_5Si_4	7.5176(4)	15.0111(9)	7.9260(5)	1.05433(9)	894.4(1)

[a] Lattice parameters of the Pu_5Rh_4-type phases are given. [b] Dominant phase.

have shown that this unusual phenomenon arises from the large magnetic exchange coupling, which is optimized in the orthorhombic phase due to a higher valence electron concentration available for metallic bonding. The studies linked cleavage of the T−T interslab bonds and, thereby, the structure of $Gd_5Si_2Ge_2$ to the number of valence electrons in the conduction band. However, this dependence is not clear-cut due to the fact that the distortion is temperature dependent and is accompanied by magnetic ordering. Moreover, while increasing the Ge amount in $Gd_5Si_2Ge_2$ without changing the electron concentration (Si and Ge are isoelectronic) results in complete breaking of the remaining T−T interslab dimers at room temperature and suppresses the coupled magnetic and structural transitions to much lower temperatures, raising the Si concentration eliminates the structural transition entirely through stabilizing the Gd_5Si_4-type structure throughout the whole temperature range.[23] In this light, a system, which can unambiguously correlate a structure to an electron concentration, was highly desirable to get a better understanding of the symmetry-breaking process in $Gd_5Si_2Ge_2$ and other related phases. Because Gd_5Ge_4 adopts two structures, a low-temperature, field-induced ferromagnetic one (Gd_5Si_4-type) with all interslab T−T dimers intact and a high-temperature paramagnetic one (Sm_5Ge_4-type) with all T−T dimers broken,[27] substituting three-valent, size-equivalent Ga (metallic radius, r_m, 1.246 Å) for four-valent Ge (r_m = 1.242 Å) in Gd_5Ge_4 could tune the interslab bonds and, thereby, induce a phase transformation through a change in the valence electron concentration. In this paper, we report on structural variations in the $Gd_5Ga_xGe_{4-x}$ system for $0 \le x \le 2.2$. Surprisingly, by tuning the valence electron concentration, we find not only a structural transformation from the Sm_5Ge_4 type to the Gd_5Si_4 one, but also a new intermediate structure, namely the orthorhombic Pu_5Rh_4 one,[28] between them, which is different from the known intermediate monoclinic structure of $Gd_5Si_2Ge_2$. Thus, this structure becomes the fourth structure type found in the R_5X_4 systems.

Experimental Section

Syntheses. The starting materials were pieces of gadolinium (99.99 wt %, Materials Preparation Center, Ames Laboratory), gallium (99.99 wt %, Aldrich), and germanium (99.999 wt %, Aldrich). The alloys with $Gd_5Ga_xGe_{4-x}$ (x = 0, 0.5, 0.6, 0.7, 0.8, 0.9, 1, 1.5, 2, 2.2, 2.5, 3) stoichiometry and a total mass of up to 3 g were prepared by arc-melting the element mixtures on a copper hearth in a 116 kPa argon atmosphere. The alloy buttons were remelted six times to ensure homogeneity (weight losses during melting were negligible, <0.1 wt %), and then one-half of each button was wrapped in tantalum foil, sealed in evacuated silica tubes, annealed at 900 °C for 20 h and quenched in cold water.

X-ray Studies. The cast and heat-treated samples were characterized by room-temperature X-ray powder diffraction (Enraf Nonius Guinier camera, Cu$K\alpha_1$, Si internal standard). The samples with $x = 0-2.2$ contained dominant Sm_5Ge_4-, Pu_5Rh_4- and Gd_5Si_4-type phases, and had $Gd_5(Ga,Ge)_3$ and Gd(Ga,Ge) impurities with the Mn_5Si_3- and CrB-type structures, respectively, which formed upon decomposition of the main phase. Moreover, although annealing improves sample crystallinity, it also increases amounts of the secondary phases. The cast and heat-treated alloys with x = 2.5 and 3 contained $Gd_3(Ga,Ge)_2$ (Gd_3Ga_2-type) and Gd(Ga,Ge) (CrB-type) phases and were not further investigated. The lattice parameters were derived from the annealed samples by the least-squares method using the CSD program package (Table 1, Figure 1).[29] Pure germanide and mixed gallide-germanides with a low Ga amount ($x = 0-0.6$) adopt a Sm_5Ge_4-type structure; the phase with a medium Ga concentration (x = 1) belong to a Pu_5Rh_4-type structure; the phases with a high Ga concentration ($x = 1.2-2.2$) crystallize in a Gd_5Si_4-type structure. Assignment of the Pu_5Rh_4-type structure to Gd_5GaGe_3 is based on the single-crystal refinement of Gd_5GaGe_3, which resulted in the interslab T1−T1 bonds of 2.93 Å that are intermediate in length as compared to those in the Sm_5Ge_4- and Gd_5Si_4-type structures.

Two R_5X_4-type phases were observed in the powders with x = 0.7, 0.8, and 0.9, indicating that the transition from the Sm_5Ge_4-type structure to the Pu_5Rh_4-type structure is a first-order one. Lattice parameters of the Pu_5Rh_4-type phase from these three samples were derived using the least-squares method and are given in Table 1. Although not all lattice parameters for the Pu_5Rh_4-type phases with x = 0.7, 0.8, 0.9 and 1 are within three standard deviations from one another, it is assumed, however, that the homogeneity range for the Pu_5Rh_4-type phase starts at x = 1 (in reality, its lower boundary can be located anywhere in the region of $0.9 \le x \le 1$ and has to be determined experimentally). Only one R_5X_4-type phase, except for the $Gd_3(Ga,Ge)_2$ and Gd(Ga,Ge) impurities, was observed in the alloys with $1 \le x \le 2.2$, thus indicating a continuous transition from the Pu_5Rh_4-

(27) Levin, E. M.; Pecharsky, V. K.; Gschneidner, K. A., Jr.; Miller, G. J. *Phys. Rev. B* **2001**, *64*, 235 103.
(28) Le Roy, J.; Moreau, J. M.; Paccard, D.; Parthe, E. *Acta Crystallogr.* **1978**, *B34*, 3315.
(29) Akselrud, L. G.; Grin, Y. M.; Pecharsky, V. K.; Zavalij, P. Y. *Kristallographiya, Suppl.*, Proceedings of 12th European Crystallographic Meet.; Academy of Sciences: Moscow, USSR, 1989; Vol. 155, pp 2−3.

Table 2. Single Crystal Data and Structure Refinement for $Gd_5Ga_xGe_{4-x}$ (*Pnma* space group, MoK_α radiation, 2θ range = 4−57°, $Z = 4$)′

composition[a]	Gd_5Ge_4	$Gd_5Ga_{0.5}Ge_{3.5}$	$Gd_5Ga_{0.7}Ge_{3.3}$	Gd_5GaGe_3	$Gd_5Ga_2Ge_2$
structure type	Sm_5Ge_4	Sm_5Ge_4	Sm_5Ge_4 88(2)% + Pu_5Rh_4 12%	Pu_5Rh_4	Gd_5Si_4
a, Å	7.683(2)	7.660(2)	7.6195(8)	7.572(2)	7.5162(7)
b, Å	14.811(4)	14.860(3)	14.838(2)	14.933(3)	14.971(1)
c, Å	7.774(2)	7.811(2)	7.8162(8)	7.884(2)	7.9149(7)
volume, Å^3	884.6(4)	889.2(3)	883.7(2)	891.5(3)	890.6(1)
R [$I > 2\sigma(I)$]	$R_1 = 0.0348$,	$R_1 = 0.0462$,	$R_1 = 0.0651$,	$R_1 = 0.0623$,	$R_1 = 0.0232$,
peak/hole, e/Å^3	2.42 / −2.69	4.79 / −2.78	7.09 / −4.59	3.17 / −2.25	1.99 / −1.32

[a] The compositions presented in the table are those of the initial samples. An EDS quantitative analysis of gallium-containing single crystals gave the following compositions: $Gd_{5.2(2)}Ga_{0.4(1)}Ge_{3.4(2)}$, $Gd_{5.2(2)}Ga_{0.6(1)}Ge_{3.2(2)}$, $Gd_{5.2(2)}Ga_{1.2(2)}Ge_{2.6(2)}$, and $Gd_{5.1(2)}Ga_{1.9(2)}Ge_{2.0(2)}$, which are within two standard deviations from the compositions of the initial samples, from which they were extracted.

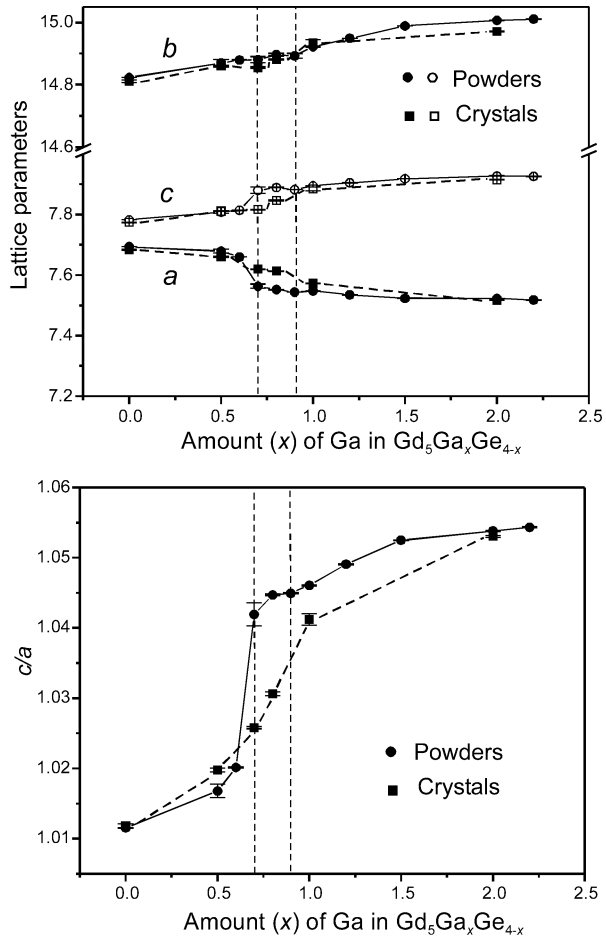

Figure 1. Lattice parameters of the $Gd_5Ga_xGe_{4-x}$ phases as a function of Ga amount. The vertical dashed lines indicate the two-phase region. Powder lattice parameters only of the Pu_5Rh_4-type structures from the two-phase region are shown. Intermediate values of the lattice parameters for single crystals from the two-phase region indicate an unusual structural behavior.

type structure to the Gd_5Si_4-type one. The argument that this transformation can be continuous (second-order) is also supported by the Landau theory (not discussed here).[30,31] Therefore, we do not define a transition point between the Pu_5Rh_4- and Gd_5Si_4-type structures. The upper boundary of the homogeneity region for the Gd_5Si_4-type phase extends, at least, to $x = 2.2$, which is its last experimentally established existence point.

Single-crystal diffraction techniques were used to confirm powder indexing results and to refine atomic parameters. Crystals were picked from the cast $Gd_5Ga_xGe_{4-x}$ samples with $x = 0$, 0.5, 0.7, 0.8, 1, 2 and checked for crystal quality by Laue photographs (Cu $K\alpha$ radiation). Room-temperature X-ray diffraction data were collected on a Bruker SMART Apex CCD diffractometer with Mo$K\alpha$ radiation and were harvested by taking three sets of 606 frames with 0.3° scans in ω and with an exposure time of 20 s per frame. The range of 2θ extended from 4° to 57°. Intensities were extracted and then corrected for Lorentz and polarization effects through the SAINT program.[32] Empirical absorption corrections were based on modeling a transmission surface by spherical harmonics employing equivalent reflections with $I/\sigma(I) > 3$ (program SADABS).[32] Structures of the crystals with $x = 0$ and 0.5 were solved by direct methods and refined on F^2 by the full-matrix least-squares method in the Sm_5Ge_4 type, and those of the crystals with $x = 1$ and 2 in the Pu_5Rh_4 and the Gd_5Si_4 types, respectively. Because Ga and Ge atoms cannot be differentiated using X-ray diffraction techniques due to one-electron difference in their electron densities, the same Ge/Ga statistical mixtures consistent with sample stoichiometries were assumed on three sites during the refinement processes. Nearest-neighbor bond distances could not be used to distinguish Ga and Ge atoms either, because similarity in atomic radii makes such analysis fruitless (metallic radii of Ga and Ge are 1.246 and 1.242 Å, respectively).[33] Unit cell dimensions and interslab T−T distances for all investigated crystals are listed in Tables 1, 2, and 3, atomic parameters and isotropic temperature factors only for the crystals with $x = 0$, 0.5, 1, and 2 are presented in Table 4, interatomic distances for the crystals with $x = 0$ and 2 are shown in Table 5 (additional crystallographic data can be obtained upon request).

Table 3. Valence Electron Concentrations (per formula unit) and Interslab T1−T1 Bond Lengths for the $Gd_5Ga_xGe_{4-x}$ Phases

	Gd_5Ge_4	$Gd_5Ga_{0.5}Ge_{3.5}$	$Gd_5Ga_{0.7}Ge_{3.3}$	Gd_5GaGe_3	$Gd_5Ga_2Ge_2$
st. type	Sm_5Ge_4	Sm_5Ge_4	Sm_5Ge_4	Pu_5Rh_4	Gd_5Si_4
electrons	31	30.5	30.3	30	29
T1−T1, Å	3.628(2)	3.500(4)	3.461(5)	2.929(7)	2.741(1)

The electron density maps for crystals with $x = 0.7$ and 0.8 were very unusual because every peak had a tail (Figure 2). Two additional crystals were picked from the samples with $x = 0.7$ and 0.8 in order to obtain precise atomic positions, but their structure solutions gave similar smeared electron density maps. Presence of a superstructure, which could account for this diffuse electron density, was not supported due to the lack of additional Bragg reflections. Because there was no indication of peak splitting, it was concluded that these crystals are merohedral twins. Treating pear-shape peaks as a superposition of two atoms belonging to two different structure types (Sm_5Ge_4 and Pu_5Rh_4) with the same lattice parameters improved the refinement process and led to lower R-values, e.g., from $R = 0.116$ to 0.065 for the crystal with $x = 0.7$. Lattice parameters for the $Gd_5Ga_{0.7}Ge_{3.3}$ crystal and atomic parameters for the dominant Sm_5Ge_4-type component are given in Tables 2 and 4.

This twinning is unusual because the two structures have the same unit cell, while preserving individual atomic arrangements. Although indirectly, the intermediate values of the lattice dimensions that fall

(30) Franzen, H. F. *Chem. Mater.* **1990**, *2*, 486.
(31) Landau, L. D.; Lifshitz, E. M. *Statistical Physics (Course of Theoretical Physics)*, 2nd ed.; Pergamon Press Ltd.: London-Paris, 1968; Vol. 5.
(32) Bruker Analytical X-ray Systems: Madison, USA, 2002.
(33) Pauling, L. C. *The Nature of the Chemical Bond and the Structure of Molecules and Crystals. An Introduction to Modern Structural Chemistry*, 3rd ed.; Cornell University Press: Ithaca, New York, 1960.

Table 4. Atomic Parameters and Isotropic Temperature Factors U_{eq} (Å^3) for Some $Gd_5Ga_xGe_{4-x}$ Phases

atom		x	y	z	U_{eq}
		Gd_5Ge_4 (Sm_5Ge_4-type)			
Gd1	8*d*	−0.02413(7)	0.60009(4)	0.17797(7)	0.0057(2)
Gd2	8*d*	0.37689(6)	0.11680(4)	0.16143(7)	0.0046(2)
Gd3	4*c*	0.20985(9)	1/4	0.49915(9)	0.0042(2)
Ge1	8*d*	0.2178(1)	0.04397(8)	0.4670(1)	0.0054(3)
Ge2	4*c*	0.0820(2)	1/4	0.1127(2)	0.0053(4)
Ge3	4*c*	0.3259(2)	1/4	0.8657(2)	0.0050(4)
		$Gd_5Ga_{0.5}Ge_{3.5}$ (Sm_5Ge_4-type)			
Gd1	8*d*	−0.01572(9)	0.59824(4)	0.18013(9)	0.0117(2)
Gd2	8*d*	0.36776(9)	0.11817(4)	0.16275(9)	0.0110(2)
Gd3	4*c*	0.2019(1)	1/4	0.5009(1)	0.0108(2)
T1	8*d*	0.2097(2)	0.04297(9)	0.4645(2)	0.0125(3)
T2	4*c*	0.0725(3)	1/4	0.1118(2)	0.0124(4)
T2	4*c*	0.3174(3)	1/4	0.8657(2)	0.0120(4)
		$Gd_5Ga_{0.7}Ge_{3.3}$ (Sm_5Ge_4-type, dominant component)			
Gd1	8*d*	−0.0155(1)	0.59773(7)	0.1802(1)	0.0090(2)
Gd2	8*d*	0.3661(1)	0.11876(7)	0.1638(1)	0.0071(2)
Gd3	4*c*	0.2006(2)	1/4	0.5019(2)	0.0070(3)
T1	8*d*	0.2083(3)	0.0424(2)	0.4643(3)	0.0090(4)
T2	4*c*	0.0712(4)	1/4	0.1118(4)	0.0087(6)
T2	4*c*	0.3168(4)	1/4	0.8655(4)	0.0074(6)
		Gd_5GaGe_3 (Pu_5Rh_4-type)			
Gd1	8*d*	0.0093(2)	0.59592(8)	0.1817(1)	0.0235(4)
Gd2	8*d*	0.3345(2)	0.12116(8)	0.1705(1)	0.0249(4)
Gd3	4*c*	0.1694(3)	1/4	0.5085(2)	0.0248(5)
T1	8*d*	0.1736(4)	0.0409(2)	0.4661(3)	0.0285(7)
T2	4*c*	0.0379(5)	1/4	0.1095(4)	0.025(1)
T2	4*c*	0.2883(6)	1/4	0.8679(4)	0.024(1)
		$Gd_5Ga_2Ge_2$ (Gd_5Si_4-type)			
Gd1	8*d*	0.01709(4)	0.59422(2)	0.18195(3)	0.0112(1)
Gd2	8*d*	0.32353(3)	0.12204(2)	0.17457(3)	0.0102(1)
Gd3	4*c*	0.15868(5)	1/4	0.51403(5)	0.0114(1)
T1	8*d*	0.16010(8)	0.04059(7)	0.46878(7)	0.0120(2)
T2	4*c*	0.0278(1)	1/4	0.1072(1)	0.0114(2)
T2	4*c*	0.2742(1)	1/4	0.8711(1)	0.0112(2)

Table 5. Interatomic Distances in $Gd_5Ga_2Ge_2$ and Gd_5Ge_4[a]

	$Gd_5Ga_2Ge_2$	Gd_5Ge_4		$Gd_5Ga_2Ge_2$	Gd_5Ge_4
atoms	distance, Å	distance, Å	atoms	distance, Å	distance, Å
T1−T1(×4)	2.741(1)	3.628(2)	T3−Gd1(×8)	3.1847(7)	3.063(1)
			Gd1(×8)	3.2264(7)	3.228(1)
T2−T3(×4)	2.631(1)	2.683(2)	Gd2(×8)	3.0943(7)	3.055(1)
			Gd3(×4)	2.957(1)	2.985(2)
T1−Gd1(×8)	3.0624(7)	2.987(1)	Gd3(×4)	3.029(1)	3.132(2)
Gd1(×8)	3.1718(7)	3.123(1)			
Gd1(×8)	3.2221(7)	3.244(1)	Gd1−Gd1(×8)	3.9095(4)	4.0013(9)
Gd1(×8)	3.5677(7)	3.613(1)	Gd1(×4)	4.0406(4)	4.072(1)
Gd2(×8)	2.9015(7)	2.881(1)	Gd2(×8)	3.7267(5)	3.529(1)
Gd2(×8)	2.9318(7)	2.913(1)	Gd2(×8)	3.8328(4)	3.790(1)
Gd2(×8)	3.0289(7)	3.003(1)	Gd2(×8)	3.9737(5)	4.453(1)
Gd3(×8)	3.1555(7)	3.062(1)	Gd2(×8)	4.1001(5)	3.932(1)
			Gd2(×8)	4.2114(5)	4.179(1)
T2−Gd1(×8)	3.2849(7)	3.199(1)	Gd3(×8)	3.6020(4)	3.5627(9)
Gd2(×8)	2.9823(7)	3.028(1)	Gd3(×8)	3.6214(4)	3.6422(9)
Gd2(×8)	3.0017(7)	3.075(1)			
Gd3(×4)	2.936(1)	2.989(2)	Gd2−Gd2(×4)	3.8312(7)	3.946(1)
Gd3(×4)	3.367(1)	3.161(2)	Gd2(×8)	3.9432(4)	4.081(1)
			Gd3(×8)	3.4991(5)	3.4632(9)
			Gd3(×8)	3.5247(5)	3.5258(9)

[a] Number of bonds per unit cell is given in parentheses.

between those of the crystals with $x = 0.5$ and 1 and with the Sm_5Ge_4- or Pu_5Rh_4-type structures, respectively, also indicate an interesting structural behavior. Presence of the two structures in single crystals is likely to result from varying the Ga/Ge ratio within the crystal. Choe et al. observed twinning of two Gd_5Ge_4- and $Gd_5Si_2Ge_2$-type phases, which are separated by a two-phase region, in single crystals of $Gd_5Si_{1.5}Ge_{2.5}$, and they traced the origin of the twinning to microscopic compositional inhomogeneity within the crystals.[34]

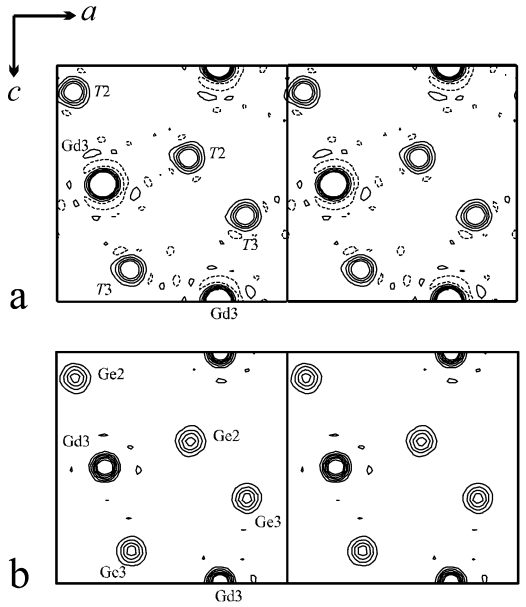

Figure 2. (a) Electron density contour map at $y = 1/4$ for $Gd_5Ga_{0.7}Ge_{3.3}$. (b) For comparison, electron density contour map at $y = 1/4$ for Gd_5Ge_4.

Results and Discussion

Structural Changes. Detailed description of the Sm_5Ge_4-, Pu_5Rh_4-, and Gd_5Si_4-type structures can be found elsewhere.[1,28,34,35] In the $Gd_5Ga_xGe_{4-x}$ system, the differentiation between the Pu_5Rh_4- and Gd_5Si_4-type structures is rather technical for the two structures have the same space groups, close lattice constants and similar atomic arrangements. The structural differences are subtle and exhibit themselves as changes in the atomic coordinates (mostly *x*), which lead to shear movement of the $_\infty{}^2[Gd_5T_4]$ slabs (T is a statistical mixture of Ga and Ge atoms on the corresponding sites) and stretching of the T1−T1 interslab bonds. And because there is a continuous transition between the Pu_5Rh_4- and Gd_5Si_4-type structures, the separation of the Pu_5Rh_4 type from the Gd_5Si_4 type is not clear-cut. To make the relationship between the structures and valence electron concentration more transparent, we treat the Pu_5Rh_4-type structure as the Gd_5Si_4-type one, in which shear movement of the slabs increases the T1−T1 interslab bonds. Thus, we will limit our analysis to the Sm_5Ge_4- and Gd_5Si_4-type structures and will emphasize only the main features of the two structures.

Both crystal structures are built from nearly identical 3^2434 nets of Gd atoms (Figure 3). Two such nets are placed over one another along the *b* axis to form two-dimensional slabs with Gd3 atoms in pseudo-cubic and T2, T3 atoms in trigonal prismatic voids. Although in the Gd_5Si_4- type (and Pu_5Rh_4-type) phases the slabs are interconnected via covalent-like T1−T1 bonds ($d_{T1-T1} = 2.74-2.93$ Å), in Sm_5Ge_4-type phases all T1−T1 interslab bonds are broken ($d_{T1-T1} = 3.46-3.68$ Å). This bond cleavage is accompanied by shear movement of the slabs along the [100] direction (Figure 4) and by increase in the corresponding lattice parameter. As judged from the relative atomic arrangements and interatomic distances (see distances

(34) Choe, W.; Miller, G. J.; Meyers, J.; Chumbley, S.; Pecharsky, A. O. *Chem. Mater.* **2003**, *15*, 1413.
(35) Holtzberg, F.; Gambino, R. J.; McGuire, T. R. *J. Phys. Chem. Solids* **1967**, *28*, 2283.

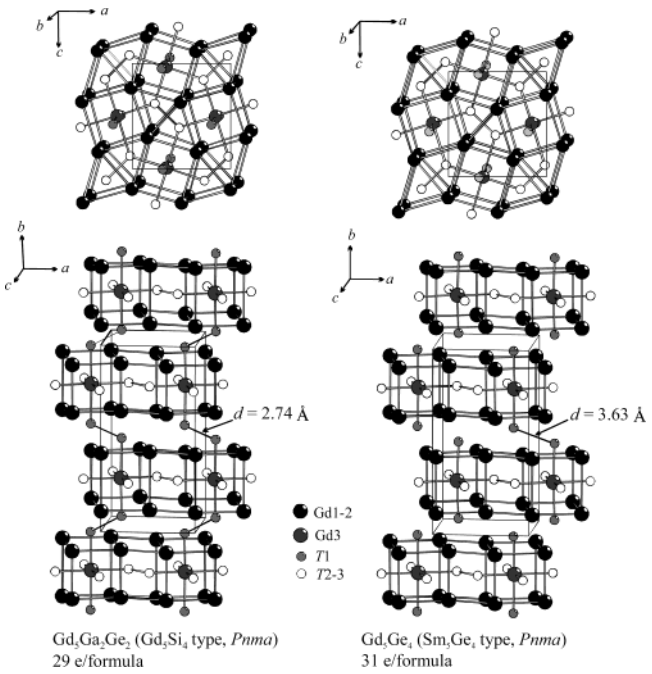

Figure 3. Crystal structures of $Gd_5Ga_2Ge_2$ and Gd_5Ge_4, projected along the *b* and *c* axes. The top projections emphasize the Gd (3^2434) nets with the Gd3 in pseudo-cubic and T2−3 in trigonal prismatic voids. In Gd_5Ge_4 the T1−T1 dimers between the slabs are broken.

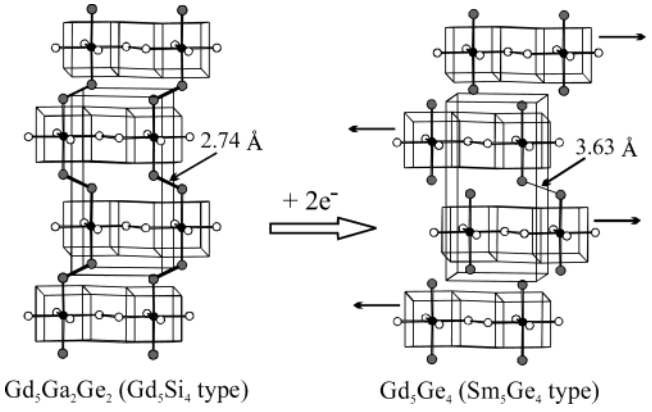

Figure 4. $Gd_5Ga_2Ge_2$ structure can be transformed into the Gd_5Ge_4 structure through shear movement of the slabs. The interslab T1−T1 dimers break as two neighboring slabs shift in the opposite directions along the *a* axis.

for $Gd_5Ga_2Ge_2$ and Gd_5Ge_4 in Table 5), structural perturbations introduced through the shear movement of the slabs are small inside the slabs but significant between the slabs. A phase transition in the $Gd_5Ga_xGe_{4-x}$ system can be monitored through the *c/a* ratio, as proposed by Choe et al. for the related phases.[34] For the powders the *c/a* ratio changes discontinuously with the Ga concentration, thus, indicating a first-order structural transformation (compare the *c/a* values at $x = 0.6$ and 0.7 in Figure 1). For the crystals, the increase in *c/a* is smoother, with the intermediate *c/a* values in the two-phase region, which is due to the unusual structural behavior of the crystals with $x = 0.7$ and 0.8, as discussed above.

One of the interesting structural features, observed in the $Gd_5Ga_xGe_{4-x}$ system, is the decrease of T1−T1 interslab bond distances with increase in the Ga amount (Table 3). There are relatively small bond changes within each structure type (~0.17 and ~0.19 Å for Sm_5Ge_4- and Gd_5Si_4-/Pu_5Rh_4-type structures, respectively) and a large change (~0.53 Å) upon the phase transition. Because the Ga and Ge atoms are similar in size but have different numbers of valence electrons, the bond cleavage must result from changes in the electronic structure. It is worth noting that at $x = 1$ a new intermediate structure is found between the Sm_5Ge_4- and Gd_5Si_4-type structures. Although the room-temperature structures in the $Gd_5Si_xGe_{4-x}$ system change from the Gd_5Si_4 to $Gd_5Si_2Ge_2$, and finally to Sm_5Ge_4 type, as *x* increases,[23] the structures in the $Gd_5Ga_xGe_{4-x}$ series evolve from the Gd_5Si_4 to Pu_5Rh_4, and finally to Sm_5Ge_4 type. Extensive literature search on the R_5X_4 family reveals that $Ce_{1.22}Sc_3Ge_4$ also has a similar T1−T1 interslab bond distance of 2.95 Å.[36]

Calculated Electronic Structure of $Gd_5Ga_2Ge_2$. To understand the relationship between the structures and valence electron concentrations, tight-binding linear-muffin-tin-orbital calculations using the atomic sphere approximation (TB-LMTO-ASA)[37] were carried out for the room-temperature structures of Gd_5Ge_4 and $Gd_5Ga_2Ge_2$. To satisfy the overlap criteria of the atomic spheres in the TB-LMTO-ASA method, empty spheres were included in the unit cell (44 in Gd_5Ge_4 and 88 in $Gd_5Ga_2Ge_2$, employing an automatic sphere generation). The 4*f* electrons of Gd were treated as core electrons, which is a good approximation due to the fact that both phases are paramagnetic at room temperature (physical properties of the $Gd_5Ga_xGe_{4-x}$ phases will be reported later).

Two structural models, consistent with the *Pnma* symmetry and sample stoichiometry, were considered for $Gd_5Ga_2Ge_2$. In the first model, the Ge atoms were placed in the T1 site and Ga atoms in T2 and T3 sites; in the second model, the Ge and Ga atoms were exchanged. Distribution of different atoms over two or more independent sites in a structure is known as a coloring problem.[38] Although electronic and geometric factors usually dictate atomic separation, the entropy contribution to the Gibbs free energy always favors statistical mixture.[39,40] In $Gd_5Ga_2Ge_2$ size effects can be neglected due to the fact that the atomic radii of Ge and Ga are similar. Therefore, distribution of Ge or Ga atoms over different sites can be qualitatively predicted by comparing total electronic energies of the two models.

In $Gd_5Ga_2Ge_2$, all the Ga and Ge atoms form either interslab T1-T1 dimers of 2.74 Å or intraslab T2-T3 dimers of 2.63 Å. According to the Zintl−Klemm electron counting formalism for valence compounds,[41] the dimers are isoelectronic with halogen dimers and carry formal negative charges of either 8 (Ga_2 dimer) or 6 (Ge_2 dimer) because no mixed dimers are present in the two structural models. If Gd atoms are considered as Gd^{3+}, then the chemical formula can be written as $(Gd^{3+})_5(Ga_2^{8-})(Ge_2^{6-})(e^-)$. The remaining electron will occupy T−T 4*p* antibonding states and also Gd−Gd and Gd−T bonding states. Because Ge is more electronegative than Ga, the 4*p* antibonding states of Ge_2 dimers are lower in energy and are more populated than those of Ga_2 dimers. Having Ge atoms on the T1 sites, which yield less disperse bands due to a larger

(36) Shpyrka, Z. M.; Bruskov, V. A.; Mokraya, I. R.; Pecharskii, V. K.; Bodak, O. I.; Zavalii, P. Y. *Izvestiya Akademii Nauk SSSR, Neorganicheskie Materialy* **1990**, *26*, 969.
(37) Andersen, O. K.; Jepsen, O. *Phys. Rev. Lett.* **1984**, *53*, 2571.
(38) Miller, G. J. *Eur. J. Inorg. Chem.* **1998**, *5*, 523.
(39) Mozharivskyj, Y.; Kaczorowski, D.; Franzen, H. F. *J. Solid State Chem.* **2000**, *155*, 259.
(40) Mozharivskyj, Y.; Franzen, H. F. *J. Alloys Compd.* **2001**, *319*, 100.
(41) Miller, G. J. In *Chemistry, Structure, and Bonding of Zintl Phases and Ions*; Kauzlarich, S. M., Ed.; VCH Publishers: New York, 1996; pp 1−59.

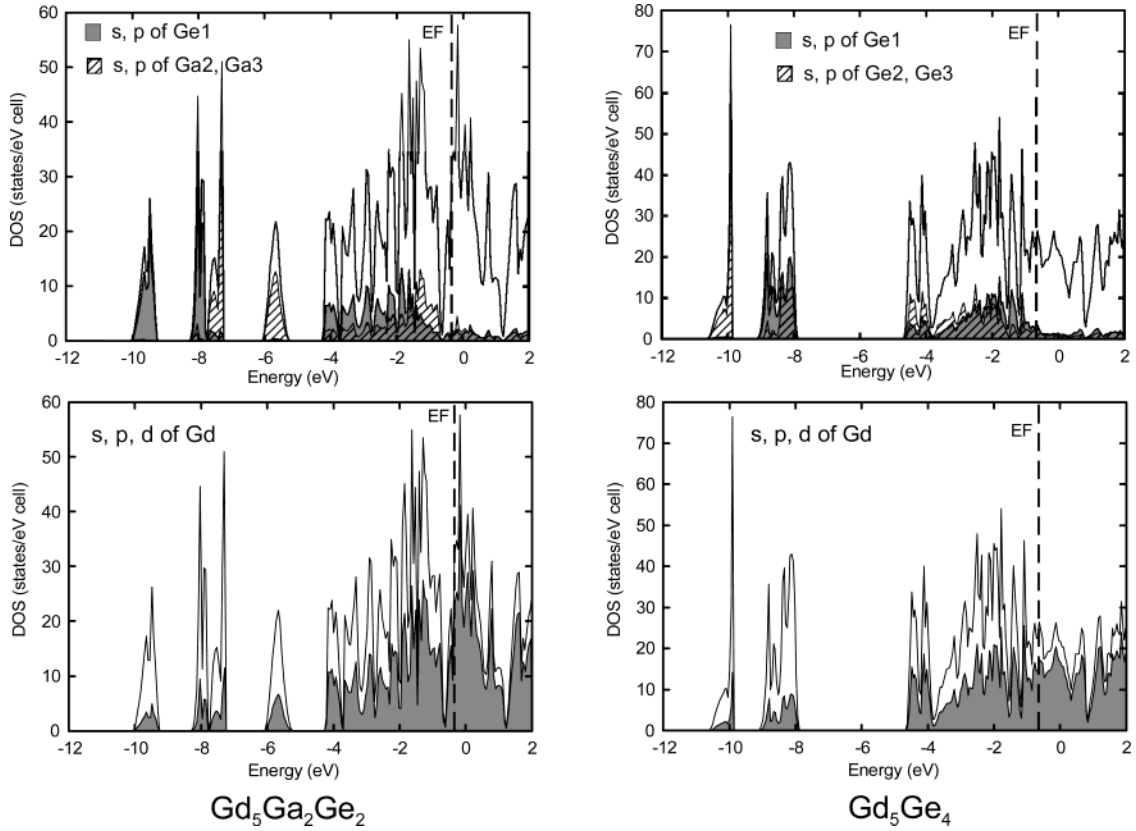

Figure 5. Total and projected densities of states (DOS) of $Gd_5Ga_2Ge_2$ and of room-temperature paramagnetic Gd_5Ge_4. In $Gd_5Ga_2Ge_2$ Ge atoms are in the T1 site, Ga atoms are in the T2 and T3 sites.

T−T separation, will result in lower electronic energy than placing Ge atoms on the T2 and T3 sites.

This simple reasoning is supported by band structure calculations. The TB-LMTO-ASA method gives lower electronic energy to the first model by 0.35 eV/unit cell, thus indicating a preference for Ge atoms at the T1 site (between the slabs) and Ga atoms at the T2 and T3 sites (inside the slabs). Calculated densities of states (DOS) and crystal orbital Hamilton population (COHP) for the two models are similar and agree well with the qualitative band structure analysis. The DOS and COHP plots for the more stable structural model of $Gd_5Ga_2Ge_2$ are presented in Figures 5 and 6. Peaks around −9.5 eV, −8 eV and −7.5 eV, −6 eV represent the bonding σ_s and antibonding σ_s* states of the Ge_2 and Ga_2 dimers, respectively, with contributions from the Gd orbitals. The conduction band can be divided into two parts by nearly a pseudo gap at −0.6 eV. The states in the lower part are derived from the 4*p* bonding states and 4*p* lone pairs of T_2 dimers that interact in a bonding manner with the Gd 6*s* and 5*d* orbitals, which are also involved in the Gd−Gd bonding. From the integration of the DOS curve, these states and the low-lying σ_s and σ_s* ones of the T_2 dimers account for 14 electron pairs per formula unit, which correlates well with the electron counting scheme used above. The states, above −0.6 eV, have the largest contribution from mostly Gd 5*d* and 6*p* orbitals, and small contribution from the antibonding σ_p* states within the T_2 dimers (intraslab Ga_2 and interslab Ge_2). Analysis of the bond characters indicates bonding Gd−Gd, Gd−Ge and Gd−Ga, nonbonding intraslab Ga−Ga and antibonding interslab Ge−Ge interactions around the Fermi level (Figure 6).

Calculated Electronic Structure of Gd_5Ge_4. Introducing more itinerant electrons into the structure of $Gd_5Ga_2Ge_2$ will significantly weaken the interslab Ge−Ge bonds but will have rather a small effect on the intraslab Ga−Ga bonds. Thus, increase in the interslab bond length is expected from electronic considerations and, indeed, is experimentally observed in the $Gd_5Ga_xGe_{4-x}$ phases upon substitution of three-valent Ga by four-valent Ge (Table 3). In Gd_5Ge_4, the interslab dimers are considered to be completely broken ($d_{Ge1-Ge1}$ = 3.63 Å). Treating the Ge monomers to be isoelectronic with noble gas atoms and to carry a formal charge of −4, we can write the chemical formula of Gd_5Ge_4 as $(Gd^{3+})_5(Ge_2^{6-})(Ge^{4-})_2(1e^-)$. Presence of the chemically different Ge^{4-} monomers with very weak interactions to other Ge^{4-} monomers affects the DOS. The two most prominent features of the DOS of Gd_5Ge_4 (Figure 5), resulting from the structural changes but not from the Ga/Ge substitution in $Gd_5Ga_2Ge_2$, are (i) appearance of an additional DOS peak around −9 eV and (ii) disappearance of the pseudogap, which in Gd_5Ge_4 should have been shifted to lower energies. (TB-LMTO-ASA calculations for Gd_5Ge_4 in the $Gd_5Ga_2Ge_2$ structure indicate the band gap shift from −0.86 eV to −1.05 eV. Lower energy of the Ge orbitals, as compared to that of the Ga orbitals, results in the gap shift.) The changes in the DOS are direct consequences of dimer breaking. Since the Ge1−Ge1 interslab interactions are weak ($d_{Ge1-Ge1}$ = 3.63 Å), the separation between the bonding σ_s and antibonding σ_s* Ge1−Ge1 states is small. While the antibonding states overlap with the antibonding states of other Ge atoms, the bonding states fall in the energy gap. Small energetic dispersion is also observed for the bonding σ_p and antibonding σ_p* Ge1−Ge1 states, with the latter moving to lower energies and, thus, eliminating the pseudogap. As in $Gd_5Ga_2Ge_2$, the remaining electron in Gd_5Ge_4 fills the bonding Gd−Gd, Gd−Ge, and

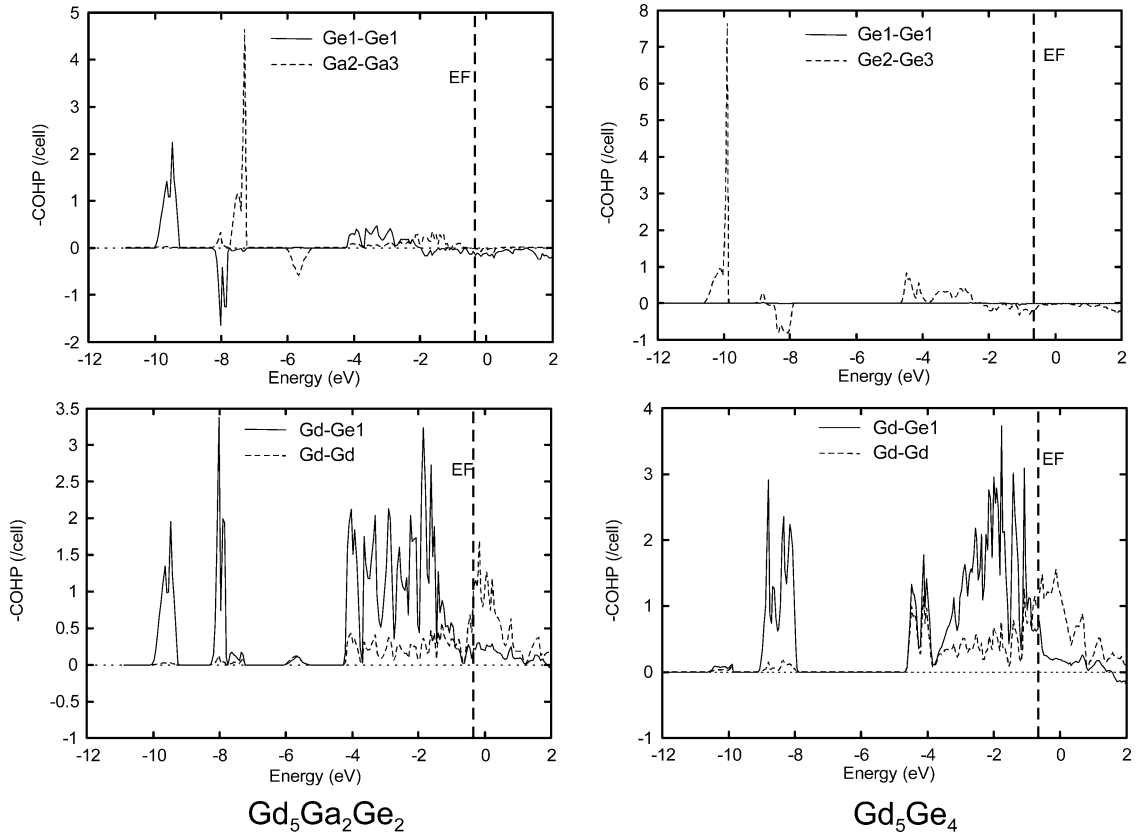

Figure 6. Crystal orbital Hamilton population (COHP) curves for some interactions in $Gd_5Ga_2Ge_2$ and in room-temperature paramagnetic Gd_5Ge_4. In $Gd_5Ga_2Ge_2$ Ge atoms are in the T1 site, Ga atoms are in the T2 and T3 sites. Interactions in the upper part are bonding, in the lower part antibonding.

antibonding intraslab Ge2−Ge3 $_{\sigma p}$* states. But, since the energy of Ge orbitals is lower than that of Ga orbitals, the antibonding σ_p* states of the dimers are now populated in Gd_5Ge_4. This argument is also valid for the Ga-containing phases, since there is always a mixture of Ga and Ge atoms on T2 and T3 sites. As a result, an increase in the T2−T3 bond distances is expected and, indeed, is experimentally observed on going from $Gd_5Ga_2Ge_2$ to Gd_5Ge_4 in the $Gd_5Ga_xGe_{4-x}$ system (see Table 5).

Reduction in the Ge1−Ge1 orbital overlap upon dimer cleavage leads to strengthening of Gd−Ge1 bonds in Gd_5Ge_4. Optimization of Gd−Ge1 interactions is intuitively expected from chemical considerations, because the Ge1 electrons, freed from bonding in the Ge_2 dimers, are donated to the Gd−Ge1 interactions. The COHP calculations support this argument. Appearance of additional states in the Gd−Ge1 bonding region from −1 eV to −0.5 eV is a direct consequence of the Ge1−Ge1 bond cleavage (Figure 6). Increase in the Gd−Ge1 bonding correlates well with the changes in the Gd−Ge1 interatomic distances: while in $Gd_5Ga_2Ge_2$, the average Gd−T1 distance is 3.1302(7) Å, in Gd_5Ge_4 the average Gd−Ge1 distance is 3.103(1) Å. Thus, there is an energetic tradeoff in interactions upon transforming the $Gd_5Ga_2Ge_2$ structure into the Gd_5Ge_4 one: while the interslab T1−T1 interactions became weaker, the Gd-T1 bonds became stronger (calculated −ICOHP values for Gd−Ge1 interactions are 5.39 and 6.46 eV/cell for the $Gd_5Ga_2Ge_2$ and Gd_5Ge_4, structures respectively).

Interestingly, the T1−T1 bond does not stretch gradually in the $Gd_5Ga_xGe_{4-x}$ system. Increase in the electron concentration by 1 e^-/formula unit results in a modest dimer stretching by ∼0.19 Å on going from $Gd_5Ga_2Ge_2$ to Gd_5GaGe_3, but introducing an extra 0.3 electron into Gd_5GaGe_3 leads to complete dimer cleavage (d_{T1-T1} = 3.46 Å) in $Gd_5Ga_{0.7}Ge_{3.3}$ and to the first-order phase transition. Further increase in the electron concentration is followed again by a small stretching (∼0.17 Å) of the T1−T1 bonds. At present, it is not fully understood why there is a sudden change in the T1−T1 interactions instead of gradual bond stretching. It can be assumed that a structure with intermediate T1−T1 distances is unstable with respect to the Pu_5Rh_4- and Sm_5Ge_4-type structures. However, the dependence of the interslab T1−T1 distances and structures themselves on the number of valence electron electrons is quite obvious in the $Gd_5Ga_xGe_{4-x}$ system: the phases with low valence electron concentrations adopt the Gd_5Si_4-type structure with T1−T1 dimers between the slabs, the phase with medium valence electron concentrations belong to the Pu_5Rh_4-type structure with intermediate interslab T1−T1 distances, and the phases with high valence electron concentrations have the Sm_5Ge_4-type structure with broken interslab T1−T1 dimers. This argument can be extended to other R_5X_4 phases and may be utilized in predicting and, subsequently, obtaining new phases. In our view, introducing extra electrons into the silicon rich $Gd_5Si_xGe_{4-x}$ compounds with the Gd_5Si_4-type structure is likely to yield phases with broken interslab bonds.

Conclusions

Structural transformations in the $Gd_5Ga_xGe_{4-x}$ system reveal an intimate relationship between the crystal structure and its valence electron concentration. Increase in electron concentration through substitution of four-valent germanium for three-valent gallium results in larger population of antibonding T1−T1 states

and, consequently, in stretching and breaking the T1−T1 interslab dimers. Dimer cleavage is accompanied by the shear movement of the slabs.

Acknowledgment. Special thanks to Prof. Vitalij K. Pecharsky for useful discussion of the results. This manuscript has been authored by Iowa State University of Science and Technology under Contract No. W-7405-ENG-82 with the U.S. Department of Energy. The research was supported by the Office of the Basic Energy Sciences, Materials Sciences Division, U.S. DOE.

Supporting Information Available: Crystallographic data relevant to the crystal structure refinement of the $Gd_5Ga_xGe_{4-x}$ single crystals. This material is available free of charge via the Internet at http://pubs.acs.org.

JA037649Z